ANESTHESIOLOGY

An Electroencephalogram Metric of Temporal Complexity Tracks Psychometric Impairment Caused by Low-dose Nitrous Oxide

Xavier C. E. Vrijdag, M.Sc., Hanna van Waart, Ph.D., Simon J. Mitchell, Ph.D., F.A.N.Z.C.A., Jamie W. Sleigh, M.D., F.A.N.Z.C.A.

Anesthesiology 2021; 134:202–18

EDITOR'S PERSPECTIVE

What We Already Know about This Topic

- Low-dose nitrous oxide is known to increase reaction time and error rate in psychometric tests, but no electrophysiologic measurement has been capable of measuring this effect

What This Article Tells Us That Is New

- A quantitative electroencephalogram analysis can identify associations between treatment with low-dose nitrous oxide and performance on psychometric tests
- Temporal complexity decreases in the medial cortical regions during nitrous oxide administration and is correlated with psychometric performance

ABSTRACT

Background: Nitrous oxide produces non–γ-aminobutyric acid sedation and psychometric impairment and can be used as scientific model for understanding mechanisms of progressive cognitive disturbances. Temporal complexity of the electroencephalogram may be a sensitive indicator of these effects. This study measured psychometric performance and the temporal complexity of the electroencephalogram in participants breathing low-dose nitrous oxide.

Methods: In random order, 20, 30, and 40% end-tidal nitrous oxide was administered to 12 participants while recording 32-channel electroencephalogram and psychometric function. A novel metric quantifying the spatial distribution of temporal electroencephalogram complexity, comprised of (1) absolute cross-correlation calculated between consecutive 0.25-s time samples; 2) binarizing these cross-correlation matrices using the median of all channels as threshold; (3) using quantitative recurrence analysis, the complexity in temporal changes calculated by the Shannon entropy of the probability distribution of the diagonal line lengths; and (4) overall spatial extent and intensity of brain complexity, was quantified by calculating median temporal complexity of channels whose complexities were above 1 at baseline. This region approximately overlay the brain's default mode network, so this summary statistic was termed "default-mode-network complexity."

Results: Nitrous oxide concentration correlated with psychometric impairment ($r = 0.50$, $P < 0.001$). Baseline regional electroencephalogram complexity at midline was greater than in lateral temporal channels (1.33 ± 0.14 bits *vs.* 0.81 ± 0.12 bits, $P < 0.001$). A dose of 40% N_2O decreased midline (mean difference [95% CI], 0.20 bits [0.09 to 0.31], $P = 0.002$) and prefrontal electroencephalogram complexity (mean difference [95% CI], 0.17 bits [0.08 to 0.27], $P = 0.002$). The lateral temporal region did not change significantly (mean difference [95% CI], 0.14 bits [–0.03 to 0.30], $P = 0.100$). Default-mode-network complexity correlated with N_2O concentration ($r = –0.55$, $P < 0.001$). A default-mode-network complexity mixed-effects model correlated with psychometric impairment ($r^2 = 0.67$; receiver operating characteristic area [95% CI], 0.72 [0.59 to 0.85], $P < 0.001$).

Conclusions: Temporal complexity decreased most markedly in medial cortical regions during low-dose nitrous oxide exposures, and this change tracked psychometric impairment.

(ANESTHESIOLOGY 2021; 134:202–18)

Downloaded from http://asa2.silverchair.com/anesthesiology/article-pdf/134/2/202/512628/20210200.0-00013.pdf by guest on 19 April 2024

Nitrous oxide is a weak anesthetic gas mostly used in dentistry, obstetrics, and acute trauma.[1] It has analgesic and hypnotic properties, as well as strong dissociative effects.[2] In the operating theater, it is used to supplement more potent anesthetic vapors in achieving general anesthesia.[3]

The electroencephalogram (EEG) and derivative anesthetic monitors have been used intensively to understand the neurologic effects of various anesthetic agents and consciousness.[4,5] Most of the research has focused on γ-aminobutyric acid–mediated (GABAergic) drugs and the transition into unconsciousness. Limited research effort has gone into understanding the narcotic effects of *N*-methyl-D-aspartate antagonists like nitrous oxide and ketamine. Various articles have shown that anesthetic depth monitors that are calibrated for GABAergic-induced unconsciousness are insensitive to nitrous oxide[6–9] due to its different

This article is featured in "This Month in Anesthesiology," page 1A. Supplemental Digital Content is available for this article. Direct URL citations appear in the printed text and are available in both the HTML and PDF versions of this article. Links to the digital files are provided in the HTML text of this article on the Journal's Web site (www.anesthesiology.org). This article has a visual abstract available in the online version.

Submitted for publication June 24, 2020. Accepted for publication October 23, 2020. Published online first on December 2, 2020. From the Department of Anaesthesiology, University of Auckland, Auckland, New Zealand (X.C.E.V., H.v.W., S.J.M., J.W.S.); the Department of Anaesthesia, Auckland City Hospital, Auckland, New Zealand (S.J.M.); and the Department of Anaesthesia, Waikato Hospital, Hamilton, New Zealand (J.W.S.).

Copyright © 2020, the American Society of Anesthesiologists, Inc. All Rights Reserved. Anesthesiology 2021; 134:202–18. DOI: 10.1097/ALN.0000000000003628

Copyright © 2020, the American Society of Anesthesiologists, Inc. Unauthorized reproduction of this article is prohibited.

mechanism of action. The EEG effects of subanesthetic concentrations of nitrous oxide have been even less well studied. Although the excellent clinical safety record of this gas precludes any necessity to develop an EEG index of its effects, nitrous oxide can be used as a scientific model to understand mechanisms of how cognition is progressively impaired by non-GABAergic sedation. Accordingly, these experiments were performed to establish methodologies—in a normobaric environment—that could later be applied to studies of hyperbaric nitrogen narcosis or other scenarios involving non-GABAergic sedation.

Nitrous oxide has been reported to cause inconsistent changes in the EEG power spectrum, but often there is an increase in power (amplitude) in high-frequency bands (>14 Hz, beta and gamma), with a relative decrease in power in the alpha and delta frequency bands (7 to 14 and 1 to 4 Hz).[10] The power reduction in alpha and delta bands[11] is localized in the frontal region[12,13] and most pronounced at higher inspired concentrations (40 to 60%).[12,14,15] Nitrous oxide also reduces spatial connectivity in parietal (at 60% N_2O) and frontal (16 to 30% N_2O) regions.[13,16] Changes in spatial connectivity are often accompanied by changes in complexity in the time domain.

Complexity is a nonspecific term used broadly to designate the use of various algorithms including Lempel–Ziv, Kolmogorov–Chaitin, a variety of different entropies, and recurrence analysis.[17] In this study, we were interested in the evolution in time of EEG motifs, because these indicate the dynamics of cortical transitions between metastable states. This "temporal complexity" has been shown to correlate with cognitive task performance,[18] and we hypothesized that nitrous oxide would reduce this. The "temporal complexity" can be measured with the diagonal line lengths calculated from recurrence plots.[19,20] These line lengths indicate the evolution of brain states over time, by their correlation between successive time samples.[18]

Therefore, in this exploratory study, we used low-dose nitrous oxide as a perturbation of cognition. Nitrous oxide is known to increase reaction time and error rate in psychometric tests.[21–24] We present a novel quantitative EEG analysis method that is sensitive to low-dose nitrous oxide exposures and correlates with the levels of psychometric impairment. The proposed analysis method quantifies the spatial distribution of the temporal complexity of the EEG signal.

Materials and Methods

Trial Design and Participants

This multidose (in randomized order), single-blind, crossover trial took place at the laboratory at Waikato Clinical School, University of Auckland, in July and August 2018. The study protocol was approved by the Health and Disability Ethics Committee, Auckland, New Zealand (reference 16/NTA/93), and was registered with the Australian New Zealand Clinical Trial Registry (registry No. U1111-1181-9722) on December 3, 2018, by S.J.M. The sample size was based on similar studies previously published.[16,22–24]

This study was a prelude to further work investigating EEG effects of gas narcosis in divers, so participants were recruited from that community. Eligible subjects were certified, healthy divers (checked with the Recreational Scuba Training Council [Jacksonville, Florida] screening questionnaire for fitness), aged between 18 and 60 yr, with normal visual acuity, either corrected or uncorrected. Exclusion criteria were the use of recreational drugs, tobacco, psychoactive medication, excessive alcohol (more than 21 standard drinks per week), or over five caffeine-containing beverages a day. All participants provided written informed consent.

Participants abstained from any caffeinated drink on the measurement day and from alcohol at least 24 h before. Participants had at least 6 h of sleep and fasted for 4 h before the measurement.

Experimental Procedures

Breathing Circuit and Monitoring. Participants were seated and breathed from a closed-circuit anesthesia loop (Vital Signs, Mexico) attached to an anesthesia machine (S/5 Aespire, Datex-Ohmeda, USA). A mouthpiece and disposable anesthetic antibacterial filter (Ultipor 25, Pall, USA) were replaced for each participant. The nose was occluded with a nose clip. The inspired fraction of oxygen, end-tidal pressure of carbon dioxide (P_{ETCO_2}), and end-tidal percentage of nitrous oxide were continuously sampled from the mouthpiece filter and were recorded every minute. Oxygen saturation and breathing frequency were monitored for participant safety.

Measurement Protocol. Every participant started with a baseline measurement while breathing 50% oxygen (balance nitrogen) on the circuit. The subjects then breathed a titrated nitrous oxide mixture (balance oxygen) to achieve an end-tidal level of 20%, 30%, or 40% N_2O, followed by 20 min of breathing air between each nitrous oxide exposure. Participants were blinded to the dose of nitrous oxide, which was administered in random order of doses dictated by a ticket drawn by the researcher when the participant arrived (order: 20-30-40%; 20-40-30%; 30-20-40%; 30-40-20%; 40-20-30%; or 40-30-20%).

Every exposure started with a 3- to 5-min wash-in period, during which the inspired fraction of nitrous oxide was manually adjusted to establish and maintain the desired end-tidal level. Then a set of measurements was undertaken consisting of EEG recording over 1 min with eyes open and 1 min with eyes closed, completion of psychometric tests, and a pupillometry measurement (pupillometry results were published elsewhere[25]). Finally, the 1-min eyes-open and -closed EEG recordings were repeated. At the end of each exposure, nitrous oxide was washed out using oxygen with a flow of 6 $l \cdot min^{-1}$ and was followed by a 20-min air breathing rest period. A final measurement set during 50%

Downloaded from http://asa2.silverchair.com/anesthesiology/article-pdf/134/2/202/512628/20210200.0-00013.pdf by guest on 19 April 2024

Copyright © 2020, the American Society of Anesthesiologists, Inc. Unauthorized reproduction of this article is prohibited.

oxygen (balance nitrogen) breathing was recorded 20 min after the last nitrous oxide exposure (fig. 1).

Outcomes

EEG Recording. The EEG was recorded using a portable active electrode 32-channel system (ActiveTwo, BioSemi, The Netherlands). The electrodes were placed in a sized cap divided over the scalp based on the international 10-10 system.[26] Two additional electrodes were placed under the eyes to record the electrooculogram to filter ocular artefacts. The offset (impedance equivalent for active systems) was checked for all electrodes, and electrode placement and gelling (SignaGel, Parker Laboratories, USA) were adjusted if the offset was above 25 μV. All signals were recorded at a sample rate of 1,024 Hz in the BioSemi Data Format (BDF) format on a laptop (Macbook Pro, Apple Inc., USA) using ActiView software (BioSemi, The Netherlands) for offline analysis. EEG was recorded continuously from the wash-in period to the last measurement for each exposure.

Three conditions were identified for analysis: tasked (while doing psychometric tests), resting-state eyes open, and resting-state eyes closed. EEG recordings taken after the psychometric tests and pupillometry (fig. 1) were used as more stable nitrous oxide levels were achieved, and fewer artefacts were present in these recordings.

Psychometric Tests. Two psychometric tests were administered on a 9.7-inch tablet computer (Galaxy Tab Active2, Samsung, South Korea). The test administration program (PenScreenSix version 2.1, Mobile Cognition Ltd., United Kingdom) stored average reaction time and number of errors made (accuracy) in each test. Two tests were selected that have shown sensitivity to narcotic effects because they test for higher-order cognitive functions.[27]

The shape-recognition test is supposed to measure the effect on short-term memory.[28] However, we found erratic results unsuitable for consistent detection of impairment, and this test was not included in our analysis.

The serial sevens test measures information processing, in particular mathematics, memory, and decision-making.[29] The participant had to decide whether the current three-digit number was the previously shown number minus seven (yes or no). The test consisted of a series of 16 descending numbers (15 questions). The maximum allowed response time per question was 10 s.

Participants attended a training session for the psychometric tests to mitigate a learning effect during the actual measurements. The tests were practiced until the results were stable.

Analysis

Data Preprocessing. The EEG data were cleaned using the FieldTrip toolbox (version c6d58e9).[30] The data for each condition and exposure were cut out of the continuous recording, rereferenced to the average, demeaned, detrended, and resampled to 256 Hz. Line (including higher harmonic) and low-frequency noise (less than 1 Hz) were filtered out. Next, independent component analysis was used to select out noise components from eye blinks, high- frequency noise, nonphysiologic noise, and bad channels. An algorithm was used to advise on the manual selection of components. The data were cut in 2-s epochs and manually inspected for remaining artefacts, with an algorithm indicating bad segments for remaining eye blinks (correlation with the electrooculogram channels) and muscle artefacts (based on high-frequency content of 105 to 120 Hz). Whole epochs were discarded if they were marked as containing artefacts. The remaining epochs for that condition and exposure were stored for further analysis. See appendix 1 for the script.

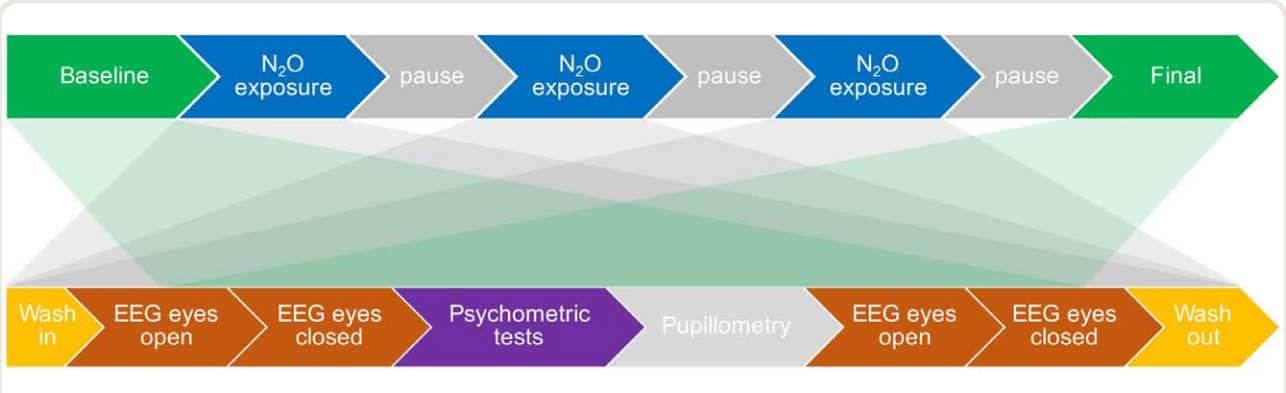

Fig. 1. The *top row* describes the order of steps during the measurement session. After preparation, a baseline measurement was conducted, directly followed by three nitrous oxide exposures with 20%, 30%, and 40% end-tidal nitrous oxide in random order, with 20-min breaks in between. The session was concluded with a final measurement. The *bottom row* describes the recording order of each step. During each measurement, the electroencephalogram (EEG), psychometric tests, pupillometry, and again EEG were recorded. Baseline and the final measurement did not have wash-in and -out steps.

Downloaded from http://asa2.silverchair.com/anesthesiology/article-pdf/134/2/202/512628/20210200.0-00013.pdf by guest on 19 April 2024

Copyright © 2020, the American Society of Anesthesiologists, Inc. Unauthorized reproduction of this article is prohibited.

Frequency Analysis. Frequency power was estimated using a multitaper Fourier transformation implemented in the FieldTrip toolbox using a Hanning window from 1 to 30 Hz in 1-Hz increments. Average per frequency band was calculated for delta (1 to 4 Hz), theta (4 to 8 Hz), alpha (8 to 14 Hz), and beta (14 to 30 Hz) bands during each exposure.

Complexity Metric. The sequence to obtain our novel complexity metric is shown in figures 2 and 3. In brief, it quantifies the variability in repeated short motifs of EEG signal over a time scale of seconds to tens of seconds (fig. 2),[18] *i.e.*, the recurrence properties of the EEG signal. Recurrence plots are widely used in physiology,[19] but when applied to EEG analysis, they provide a graphical indication of periods when a section of the EEG signal is similar to subsequent sections. The presence of a long diagonal line in the recurrence plot indicates a slowly evolving similarity in EEG pattern (*i.e.*, to produce a diagonal line, the motif at time = 1 is similar to that at time = 2, and the motif at time = 3 is similar to that of time = 2). Blocks of high correlation (yellow in fig. 3B) are stable periods. The standard recurrence plot summary statistic (Shannon entropy of the diagonal line length) can be seen as a measure of the variation in the duration of metastable states, *i.e.*, the temporal complexity of the signal for each channel. A high entropy suggests the presence of a mixture of slowly evolving metastable brain states, coexistent with short-lived brain states. As seen in the histograms of figure 3C, a low entropy is indicative of predominantly short-lived recurrences. To condense this into a single spatial summary statistic for the whole scalp, we found the median complexity of a subset of high-complexity channels. This subset of channels was found to roughly overlie the default mode network. This is in agreement with previous work showing that the default mode network has high complexity based on its critical functional role in resting-state networks.[31] The following steps give the metric:

1. To obtain the motifs, the EEG signals were split into samples of 0.25-s duration. For each channel, the absolute values of the Pearson correlations between all of these 0.25-s samples were calculated (fig. 3A).[18]
2. The median value of Pearson correlation over all channels and cross-correlations of the baseline exposure was taken as the threshold to produce a dichotomized matrix for the recurrence analysis (fig. 3B).
3. The Shannon entropy of the probability distribution of the diagonal line lengths[32] for each channel was calculated to capture the variability in temporal changes (fig. 3C).
4. A region of interest was defined as the electrodes with a complexity value larger than 1 at baseline. As described above, based on the regional distribution of our results, we named the spatial distribution of the temporal complexity metric, "default-mode-network complexity." The metric was calculated for each exposure and condition (tasked, eyes open, eyes closed) as the median of the complexity of the electrodes in the set region of interest (red-encircled area in fig. 3D).

The results were robust to a range of differing trialed values for the sample length, dichotomization threshold, and region-of-interest threshold (results not shown). See appendix 2 for the script. Regional complexity was calculated by taking the mean of the Shannon entropy of the channels of that region.

Psychometric Test Analysis. A combined psychometric-impairment metric (scaled 0 to 1) was calculated using both

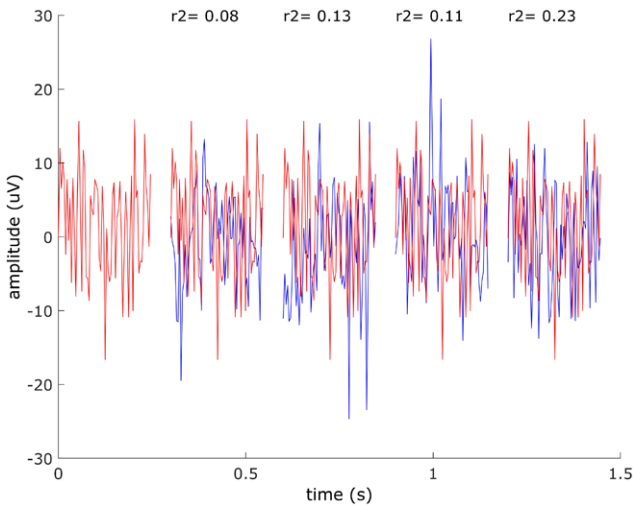

Fig. 2. A reference sample of 0.25-s electroencephalogram data of one channel (*red*), followed by four samples of the same channel (*blue*), with their absolute correlation. These temporal correlation values construct the correlation matrix in figure 3A.

Downloaded from http://asa2.silverchair.com/anesthesiology/article-pdf/134/2/202/512628/20210200.0-00013.pdf by guest on 19 April 2024

Copyright © 2020, the American Society of Anesthesiologists, Inc. Unauthorized reproduction of this article is prohibited.

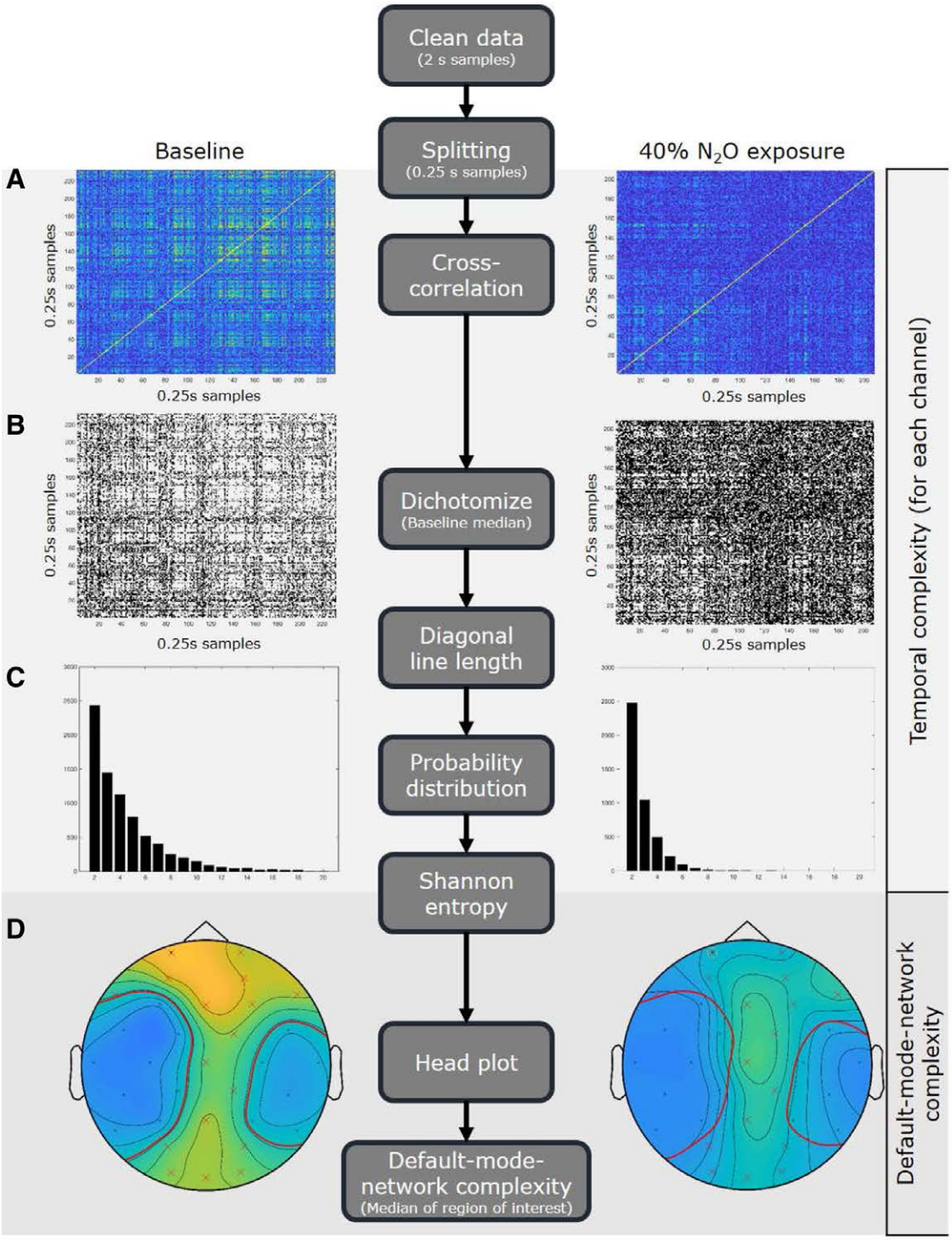

Fig. 3. Flow diagram of the analysis algorithm in the *middle*. On the *left*, the intermediate results of the algorithm are shown of participant 1 (table 1) during the baseline measurement. On the *right* are the results of the same participant during the 40% end-tidal nitrous oxide exposure. *A–C* are from the signals of the Fp1 electrode (*yellow circle* in *D*). The analysis steps are repeated for each channel separately. (*A*) Absolute cross-correlation values (*blue*, low; *yellow*, high) between the electroencephalogram samples. (*B*) Dichotomized results (0, *black*; 1, *white*). (*C*) Probability distributions of the diagonal line lengths. (*D*) Surface head plot with contour lines of the Shannon entropy for all electrodes, showing the spatial distribution of temporal complexity (*blue*, low; *yellow*, high). The *red line* indicates the contour with value 1, in which the electrodes with a value above 1 at baseline (in *yellow*/*green*) are enclosed (*red* ×). This selection is consistent over exposures and forms the region of interest for the electroencephalogram default-mode-network complexity analysis.

Downloaded from http://asa2.silverchair.com/anesthesiology/article-pdf/134/2/202/512628/20210200.0-00013.pdf by guest on 19 April 2024

Copyright © 2020, the American Society of Anesthesiologists, Inc. Unauthorized reproduction of this article is prohibited.

the mean reaction time and error rate to counteract the speed-accuracy trade-off (equation 1).[33]

$$\frac{\frac{mean\ reaction\ time}{max\ respons\ time}+\frac{number\ of\ errors}{number\ of\ questions}}{2} \quad (1)$$

Statistical Analysis

All data were analyzed with Matlab version 2018a (Mathworks, USA) except the carbon dioxide data, which were analyzed with SPSS version 25 (IBM, USA). The idea of EEG data analysis using temporal complexity was preplanned, based on previous published work.[20,34,35] However, the specific values of various parameters in the algorithm and the default mode network region of interest were data-driven, as part of the exploratory study. The comparison between the EEG metric and psychometric test score was predefined. All outcome measures were tested for normality and subsequently characterized by their mean and SD. Comparisons of regional complexity were done using a two-tailed paired *t* test and reported as mean difference and 95% CI. *P* values were regarded as significant at $P < 0.05$, with Bonferroni correction for multiple comparisons.

For all exposures and individuals, a linear mixed-effects model was used to calculate the relationship between the EEG default-mode-network complexity metric (*DMNcomplexity*) and the psychometric test metric (*S77*) using equation 2.

$$S77 \sim 1+DMNcomplexity+(1+DMNcomplexity|\ participant) \quad (2)$$

The between-participant variation was included as a random effect, with a random intercept and slope. This design can capture variation in baseline complexity and dose response for each subject. The models for the three conditions were compared using a likelihood ratio test with 1,000 simulations.

To research the possible influence of hypercapnia, carbon dioxide levels were analyzed. The P_{ETCO_2} value at the start of the psychometric test was added as a fixed-effect parameter to the mixed-effects model for the tasked condition (EEG recording during the psychometric test). This model was compared to the model without carbon dioxide level (same method as above).

The influence of the power in each frequency band (delta [1 to 4 Hz], theta [4 to 8 Hz], alpha [8 to 14 Hz], beta [14 to 30 Hz], and gamma [30 to 45 Hz]) on the final model was also investigated. For this subanalysis, the EEG data of the eyes-open condition were bandpass-filtered with a Butterworth filter (order 4) in both directions using a Hamming window for each frequency band.

A receiver operating characteristic analysis was used to compare the default-mode-network complexity metric against the serial sevens test results. The serial sevens data were dichotomized to "impaired" (greater than 0.16) and "not impaired" (less than or equal to 0.16), based on the upper value of the interquartile range (fig. 4) of the baseline exposure.

Results

The 12 participants (8 male), aged between 23 and 55 yr (mean. 36 yr), had an average body mass index of 26.3 kg/m^2 (22.7 to 31.3). On average, 1.7 of 30, 1.3 of 30, and 19.5 of 108 (eyes open, eyes closed, and tasked, respectively) of the 2-s EEG samples were removed due to artefacts. The latter were mostly muscle artefacts. EEG frequency analysis shows an increase in power in the beta band, with a relative decrease in the delta band, most prominent in the frontal region and most visible in the 20% and 40% exposures (Supplemental Digital Content 1, http://links.lww.com/ALN/C512, shows the frequency band analysis). This is similar to previous studies.[10–14] In general, the serial sevens test results worsened (fig. 4A) and the complexity metric decreased (fig. 4B) at increased end-tidal concentrations of nitrous oxide, particularly once the 40% concentration was reached. End-tidal nitrous oxide concentrations exhibited a moderate correlation with both the serial sevens scores and the EEG default-mode-network complexity ($r = 0.50$, $P < 0.001$ and $r = -0.55$, $P < 0.001$, respectively).

Regional Differences

At baseline (fig. 5), regional temporal complexity was greater in the midline (1.33 ± 0.14 bits), which approximately overlies the default mode network, than in channels overlying lateral temporal brain regions (0.81 ± 0.12 bits; mean difference, 0.52 [0.39 to 0.65], $P < 0.001$). Increasing nitrous oxide exposure caused a decrease in brain complexity predominantly in the midline (baseline *vs.* 40% N_2O: mean difference, 0.20 bits [0.09 to 0.31], $P = 0.002$) and prefrontal (baseline *vs.* 40% N_2O: mean difference, 0.17 bits [0.08 to 0.27], $P = 0.002$) regions, whereas complexity in the lateral temporal region did not change significantly (baseline *vs.* 40% N_2O: mean difference, 0.14 bits [−0.03 to 0.30], $P = 0.100$). These changes were reversed after cessation of nitrous oxide.

Mixed-effects Modeling

At baseline, the EEG default-mode-network complexity metric ranged from 1.13 to 1.38 bits between subjects. The effects of the different doses of nitrous oxide were variable between subjects. For some participants, the ranking order of the nitrous oxide concentrations did not correlate with the ranking order of both the psychometric tests (y axis) and EEG default-mode-network complexity (x axis; fig. 6). There was a significant difference between the models for only the eyes-closed *versus* tasked conditions ($P = 0.003$), but the log likelihoods of the models for the three conditions were very similar (52.3, 47.4, and 42.7). Therefore, figure 7 shows the results of the model based on the eyes-open data.

Downloaded from http://asa2.silverchair.com/anesthesiology/article-pdf/134/2/202/512628/20210200.0-00013.pdf by guest on 19 April 2024

Copyright © 2020, the American Society of Anesthesiologists, Inc. Unauthorized reproduction of this article is prohibited.

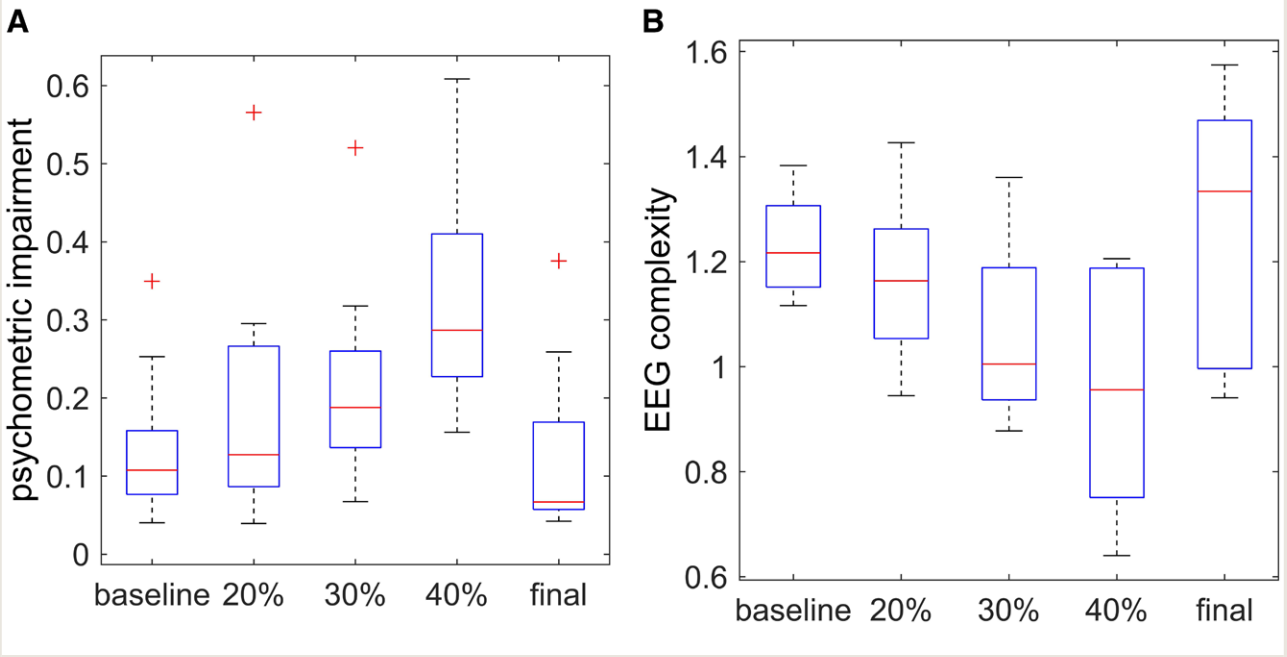

Fig. 4. *Box plots* of the serial sevens test results (reaction time and accuracy) combined metric (*A*) and electroencephalogram (EEG) default-mode-network complexity metric (in bits; *B*). Both box plots show the median (*red line*), interquartile range (*blue box*), and the *whiskers* indicating the full range of the data. Outliers (*red +*) are values larger than 1.5 times the interquartile range.

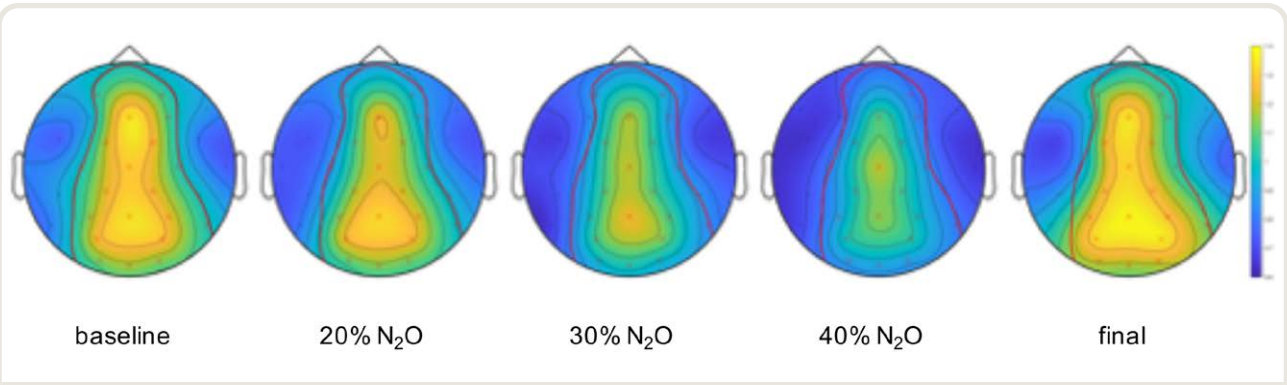

Fig. 5. Average surface head plots with contour lines of the Shannon entropy (in bits) for all electrodes (*blue*, low; *yellow*, high) for each of the exposures of all participants. The *red line* indicates the contour with a value of 1, in which the electrodes with a value above 1 at baseline are enclosed (*red* ×).

At an individual level, for each subject there was a significant linear trend between the EEG default-mode-network complexity metric and cognitive decline (fig. 6 blue lines and table 1). The goodness of fit of the model was confirmed by a good agreement with fitted *versus* measured values (fig. 7A, $r^2 = 0.67$) and lack of autocorrelation in the residuals (fig. 7B). On average, psychometric impairment increased 10% with every 38% decrease in EEG default-mode-network complexity. The receiver operating characteristic curve of the complexity metric *versus* the serial sevens test showed an area under the curve of 0.72 (95% CI, 0.59 to 0.85; $P < 0.001$; fig. 8).

P_{ETCO_2} was within normal ranges at group level (5.5 ± 0.6 kPa [41 ± 4.5 mmHg]), and there was no significant difference between exposures. However, some participants were above normal (greater than 5.7 kPa [43 mmHg]) at the start of the psychometric test. The addition of P_{ETCO_2} values as a fixed effect in the model did not change the results ($P = 0.460$). The frequency subanalysis revealed that there was no specific frequency band driving the default-mode-network complexity (results not shown).

Downloaded from http://asa2.silverchair.com/anesthesiology/article-pdf/134/2/202/512628/20210200.0-00013.pdf by guest on 19 April 2024

Copyright © 2020, the American Society of Anesthesiologists, Inc. Unauthorized reproduction of this article is prohibited.

Discussion

In this exploratory study, our novel complexity metric tracked psychometric impairment during low-dose nitrous oxide exposure. The EEG default-mode-network complexity metric is a simple and fast algorithm that incorporates two main concepts: cross-correlation–based recurrence quantification analysis[32] and specific regional changes.[36]

High-level Cognition Requires Sustained Recurrence

For each channel, we calculated the complexity of that signal by determining the correlation between short successive EEG samples. The concept behind this is that if there is a high correlation over time, the EEG signal is repeating itself, indicating the presence of prolonged or similar metastable brain states. Variation in runs of repetition of EEG patterns is seen as an increase in the variability of diagonal line lengths in the recurrence plots and consequently an increase in the Shannon entropy of these plots (also seen as an increase in width of the histograms; fig. 3C). The increased entropy of the recurrences is thus primarily driven by many periods of prolonged (more than approximately 1,000 ms) EEG similarity, which widen the recurrence histograms. The neurophysiologic correlates of this pattern are not well defined, but it is well established that conscious perceptions are associated with ignition of sustained (more than 250 ms) neural activity[37] and prolonged (more than approximately 1,000 ms) complex responses to transcranial magnetic stimulation.[38] Although our study does not look at the transition to unconsciousness, we can speculate that inability of

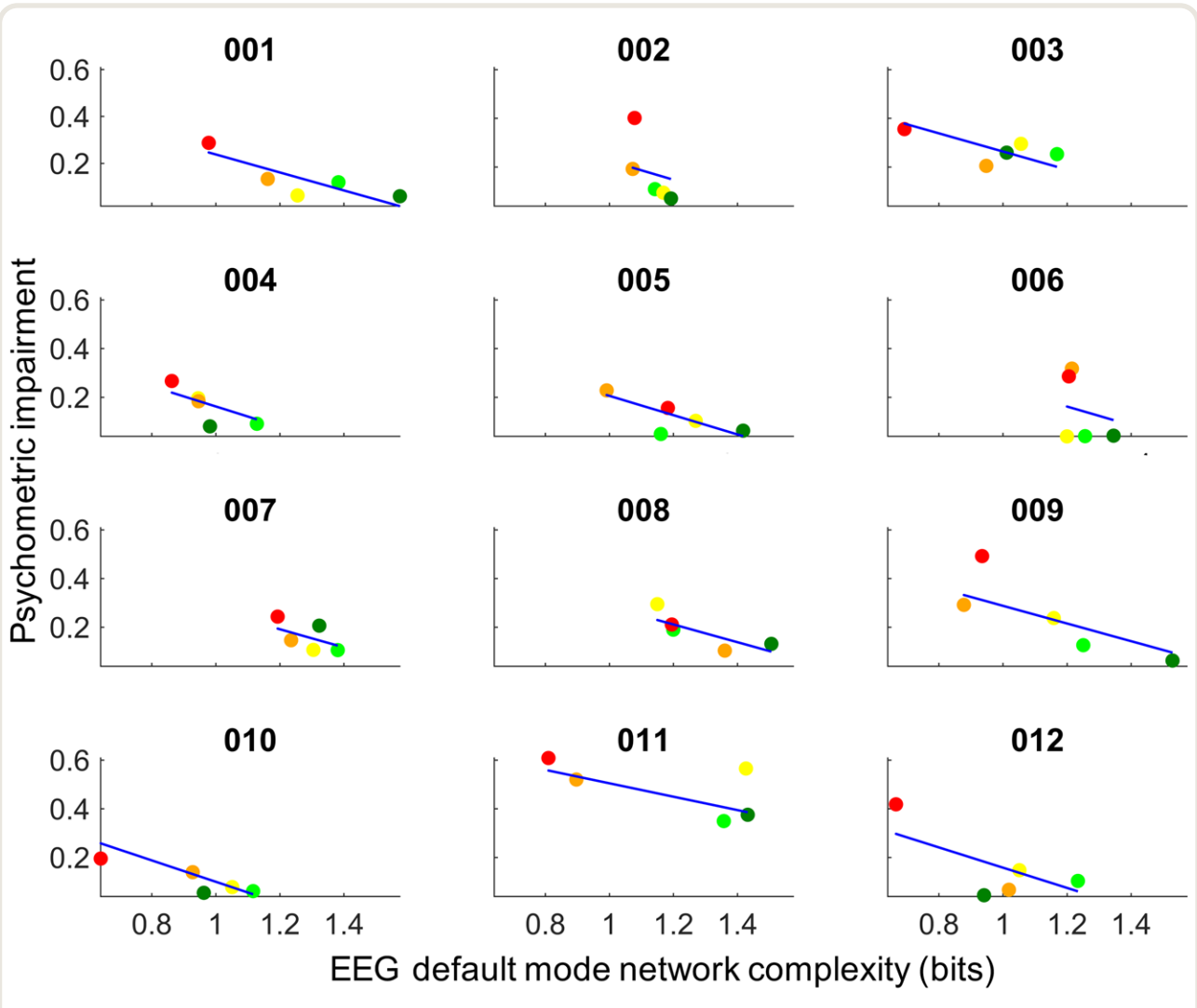

Fig. 6. Electroencephalogram (EEG) default-mode-network complexity (in bits) *versus* psychometric impairment for each subject. *Colored dots* depict each nitrous oxide concentration: *light green* shows baseline, *dark green* shows final, *yellow* shows 20%, *orange* shows 30%, and *red* shows 40%. *Blue lines* are the fitted model.

Downloaded from http://asa2.silverchair.com/anesthesiology/article-pdf/134/2/202/512628/20210200.0-00013.pdf by guest on 19 April 2024

Copyright © 2020, the American Society of Anesthesiologists, Inc. Unauthorized reproduction of this article is prohibited.

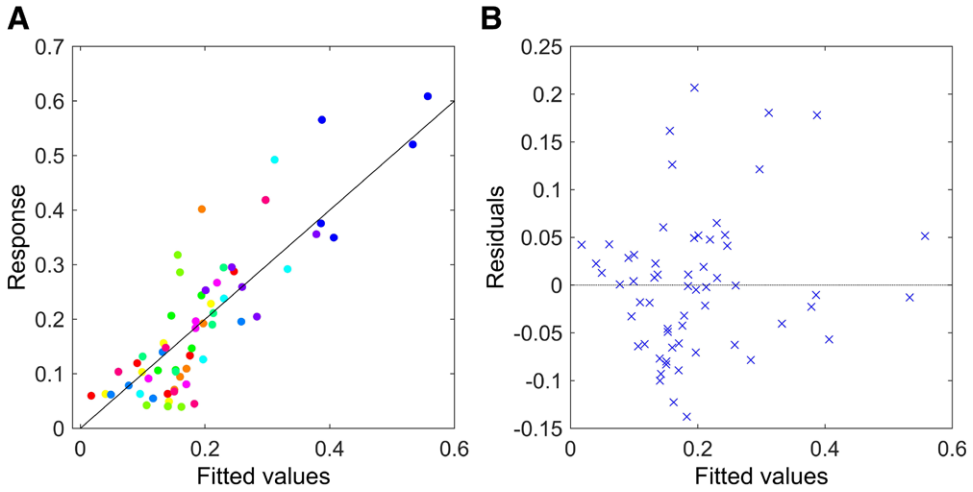

Fig. 7. Graphs showing the results of the linear mixed-effect model based on the electroencephalogram data during eyes open at the end of each measurement *versus* the serial sevens psychometric test results (response). (*A*) Estimated psychometric test values based on the electroencephalogram default-mode-network complexity (from the model) *versus* the actual psychometric test results. Each color represents the data of a single participant. (*B*) Fitted results *versus* the residuals.

Table 1. Individual Subject Intercept and Slope from the Eyes-open Linear Mixed-effect Model (95% CI)

Participant	Intercept	Slope
1	0.62 (0.57 to 0.67)	−0.38 (−0.42 to −0.35)
2	0.61 (0.56 to 0.66)	−0.39 (−0.42 to −0.35)
3	0.64 (0.58 to 0.69)	−0.37 (−0.41 to −0.34)
4	0.58 (0.52 to 0.63)	−0.41 (−0.45 to −0.38)
5	0.60 (0.55 to 0.65)	−0.40 (−0.43 to −0.36)
6	0.62 (0.57 to 0.67)	−0.38 (−0.42 to −0.35)
7	0.64 (0.59 to 0.69)	−0.37 (−0.41 to −0.34)
8	0.65 (0.60 to 0.70)	−0.36 (−0.40 to −0.33)
9	0.65 (0.60 to 0.70)	−0.36 (−0.40 to −0.33)
10	0.54 (0.49 to 0.59)	−0.44 (−0.48 to −0.40)
11	0.78 (0.73 to 0.83)	−0.28 (−0.31 to −0.24)
12	0.57 (0.52 to 0.63)	−0.42 (−0.45 to −0.38)

the brain to sustain recurrence patterns is a signature of loss of diversity of metastable states, which seems to be an indication of impairment of higher-level function.

This first part of our analysis method utilizes methodologies that originate from recurrence quantification analysis, but in our study, these methodologies were applied to cross-correlation plots.[18] These methods quantify nonlinear dynamic phenomena.[19] Based on the global neuronal workspace hypothesis, normal cognitive performance could be associated with recurrence loops for two reasons.[37] First, recurrence loops can help cortical processors sustain a signal, and hence the information can be maintained in the working memory. Second, by recurrent excitation, a signal can be amplified, helping information sharing between cortical processors. Hence, a certain amount of recurrence is needed to sustain normal cognitive functioning. However, it is unclear whether the EEG recurrence is driven by local or global reverberant networks. In the neuroscience field, recurrence analysis has been utilized in epilepsy detection,[39] sleep-stage recognition,[40,41] and depth of anesthesia detection.[35,42,43] However, the depth-of-anesthesia articles all report results with GABAergic agents, whereas our study used an *N*-methyl-D-aspartate antagonist.

Regional Variation

The other observation from this work is the marked difference in regional baseline complexity and the regional effect of the nitrous oxide. Prefrontal and midline regional complexity reduced under nitrous oxide exposure, whereas complexity of the lateral fronto/temporal/parietal regions showed relatively minor change.The serial sevens test requires coordination of several cognitive tasks, *e.g.*, mathematics, memory, and decision-making,[29] which were impaired by nitrous oxide. The regional differences correlate well with the concept of the fragmentation of selfhood,[36] where higher-order thinking (affected in our study) is primarily located at the (pre)frontal region, whereas the sentience and salience (located in the temporal/insular region) are less affected by low-dose nitrous oxide. Numerous studies have supported this division of functions in the brain, all concluding that higher cognitive functions are predominantly located in the (pre)frontal region and with their connections to posterior medial regions.[44,45] Similar reductions in frontal connectivity have been found during subanesthetic ketamine exposure.[46]

A recent study showed a significant decrease in EEG network connectivity (lagged phase coherence) induced by

Downloaded from http://asa2.silverchair.com/anesthesiology/article-pdf/134/2/202/512628/20210200.0-00013.pdf by guest on 19 April 2024

Copyright © 2020, the American Society of Anesthesiologists, Inc. Unauthorized reproduction of this article is prohibited.

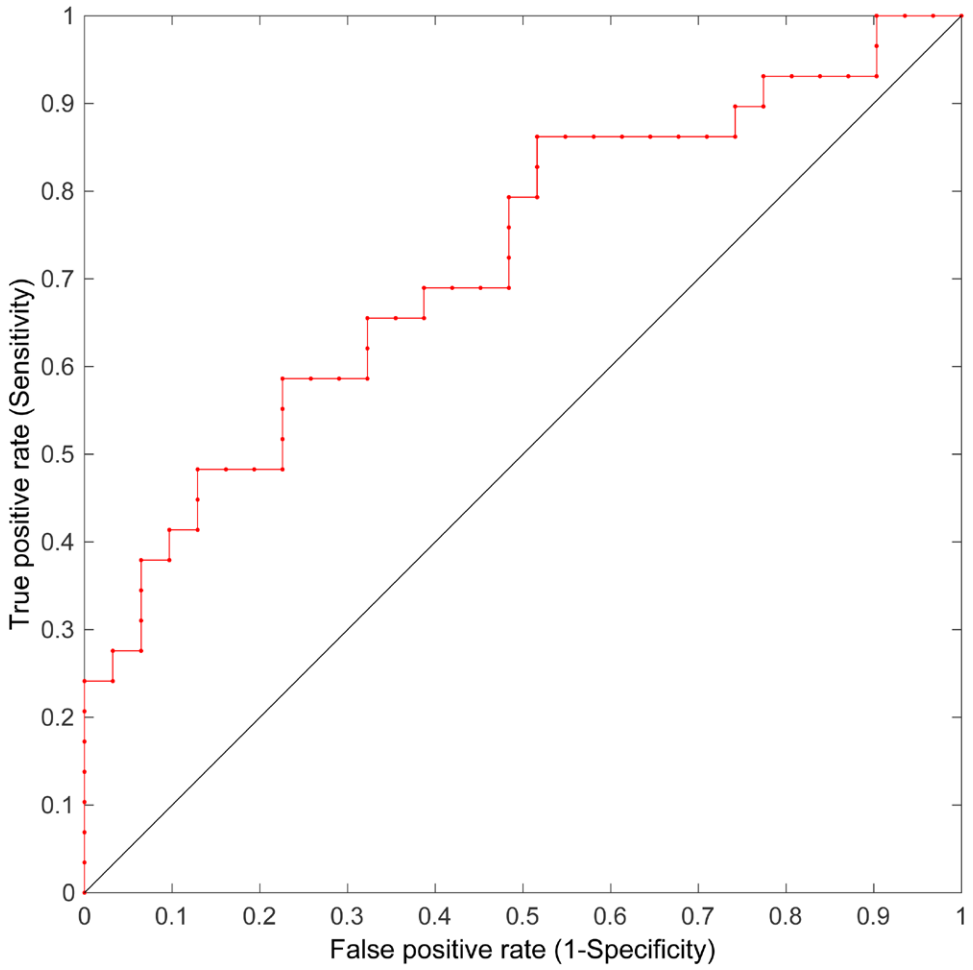

Fig. 8. Receiver operating characteristic graph comparing the sensitivity and specificity of the electroencephalogram default-mode-network complexity calculated with the eyes open at the end of the measurement *versus* the results of the serial sevens psychometric test.

50% inhaled nitrous oxide.[47] This disruptive effect of relatively high-dose nitrous oxide on the flow of information between brain regions is consistent with the default mode network regional decrease in complexity found in our study. The nitrous oxide–impaired cognitive performance was strongly associated with loss of complexity in the medial default mode network regions (the so-called "hot zone").[38] The exact role of these brain regions (precuneus, posterior, and anterior cingulate cortices) is still intensely debated,[48] but seems to be more closely aligned with overall higher-order brain integration and coordination[49] rather than specific tasks. In particular, activity is associated with semantic processing and memory retrieval, which are necessary for the serial sevens test.[50]

Limitations

Our study had some strengths. It was performed in a laboratory where the environment was well controlled to optimize the EEG recording, with full-scalp 32 channels. By controlling the end-tidal concentrations of nitrous oxide, we were able to control the exposure to a narcotic agent precisely at three distinct levels, without the interference of other drugs. However, the psychometric tests showed a high level of personal variability in participants' responses to nitrous oxide. The variability could be explained by a carryover or learning effect between the exposures, although we did incorporate a 20-min pause between exposures and randomized the order of exposures to minimize this effect. We measured end-tidal carbon dioxide and found that an increased P_{ETCO_2} above a normal value of 5.7 kPa (43 mmHg), which was found in some participants/exposures, did not contribute to the narcotic effects found, similar to the results of Foster and Liley.[11]

Our study also had some weaknesses. First, the participant group was relatively small. In mitigation, it was reassuring that the EEG default-mode-network complexity

Downloaded from http://asa2.silverchair.com/anesthesiology/article-pdf/134/2/202/512628/20210200.0-00013.pdf by guest on 19 April 2024

Copyright © 2020, the American Society of Anesthesiologists, Inc. Unauthorized reproduction of this article is prohibited.

metric consistently decreased in every subject as psychometric impairment increased. Second, our exploratory analysis was directed toward a time-domain analysis. We did not use source localization to refine the locations of temporal complexity further; hence, we chose to use general descriptors of locations. This increased the speed of analysis, kept the analysis method simple, and avoided the assumptions underlying all source localization methods. We also acknowledge that our limited spatial resolution means that we have used the term "default-mode-network complexity" as a descriptive shorthand rather than being able to establish its full anatomical detail.

In conclusion, our novel quantitative EEG default-mode-network complexity metric based on temporal complexity is sensitive to psychometric impairment caused by low-dose nitrous oxide. However, further research is needed to evaluate its functionality, because this was an exploratory study. If robust, this algorithm may be useful in quantifying and studying mild narcosis in situations where patients are less self-aware due to the dissociative effects of nitrous oxide or other non-GABAergic sedatives.

Acknowledgments

The authors are grateful to all participants in this study. Furthermore, the authors acknowledge Jonathan Termaat, Dip.R.N., Gay Mans, N.Z.R.G.O.N., Amy Gaskell, M.B.Ch.B., F.A.N.Z.C.A. (all Department of Anaesthesia, Waikato Hospital, Hamilton, New Zealand), Rebecca Pullon, Ph.D., and Marta Seretny, M.D., M.P.H., Ph.D., F.R.C.A. (both Department of Anaesthesiology, University of Auckland, Auckland, New Zealand), for their support during the data collection.

Research Support

This study was supported by funding from the Office for Naval Research Global (Tokyo, Japan), U.S. Navy grant No. N62909-18-1-2007.

Competing Interests

The authors declare no competing interests.

Reproducible Science

Full protocol available at: x.vrijdag@auckland.ac.nz. Raw data available at: x.vrijdag@auckland.ac.nz.

Correspondence

Address correspondence to Mr. Vrijdag: School of Medicine, University of Auckland, Private Bag 92019, Auckland 1142, New Zealand. x.vrijdag@auckland.ac.nz. This article may be accessed for personal use at no charge through the Journal Web site, www.anesthesiology.org.

References

1. O'Sullivan I, Benger J: Nitrous oxide in emergency medicine. Emerg Med J 2003; 20:214–7
2. Brown EN, Purdon PL, Van Dort CJ: General anesthesia and altered states of arousal: A systems neuroscience analysis. Annu Rev Neurosci 2011; 34:601–28
3. Myles PS, Leslie K, Silbert B, Paech MJ, Peyton P: A review of the risks and benefits of nitrous oxide in current anaesthetic practice. Anaesth Intensive Care 2004; 32:165–72
4. Marchant N, Sanders R, Sleigh J, Vanhaudenhuyse A, Bruno MA, Brichant JF, Laureys S, Bonhomme V: How electroencephalography serves the anesthesiologist. Clin EEG Neurosci 2014; 45:22–32
5. Kaiser HA, Hight D, Avidan MS: A narrative review of electroencephalogram-based monitoring during cardiovascular surgery. Curr Opin Anaesthesiol 2020; 33:92–100
6. Rampil IJ, Kim JS, Lenhardt R, Negishi C, Sessler DI: Bispectral EEG index during nitrous oxide administration. Anesthesiology 1998; 89:671–7
7. Barr G, Jakobsson JG, Owall A, Anderson RE: Nitrous oxide does not alter bispectral index: Study with nitrous oxide as sole agent and as an adjunct to i.v. anaesthesia. Br J Anaesth 1999; 82:827–30
8. Anderson RE, Jakobsson JG: Entropy of EEG during anaesthetic induction: A comparative study with propofol or nitrous oxide as sole agent. Br J Anaesth 2004; 92:167–70
9. Voss L, Sleigh J: Monitoring consciousness: The current status of EEG-based depth of anaesthesia monitors. Best Pract Res Clin Anaesthesiol 2007; 21:313–25
10. Purdon PL, Sampson A, Pavone KJ, Brown EN: Clinical electroencephalography for anesthesiologists: Part I: Background and basic signatures. Anesthesiology 2015; 123:937–60
11. Foster BL, Liley DT: Nitrous oxide paradoxically modulates slow electroencephalogram oscillations: Implications for anesthesia monitoring. Anesth Analg 2011; 113:758–65
12. Foster BL, Liley DT: Effects of nitrous oxide sedation on resting electroencephalogram topography. Clin Neurophysiol 2013; 124:417–23
13. Pelentritou A, Kuhlmann L, Cormack J, Mcguigan S, Woods W, Muthukumaraswamy S, Liley D: Source-level cortical power changes for xenon and nitrous oxide–induced reductions in consciousness in healthy male volunteers. Anesthesiology 2020; 132:1017–33
14. Pelentritou A, Kuhlmann L, Cormack J, Woods W, Sleigh J, Liley D: Recording brain electromagnetic activity during the administration of the gaseous anesthetic agents xenon and nitrous oxide in healthy volunteers. J Vis Exp 2018; 131:56881
15. Kuhlmann L, Liley DTJ: Assessing nitrous oxide effect using electroencephalographically-based depth of

Downloaded from http://asa2.silverchair.com/anesthesiology/article-pdf/134/2/202/512628/20210200.0-00013.pdf by guest on 19 April 2024

Copyright © 2020, the American Society of Anesthesiologists, Inc. Unauthorized reproduction of this article is prohibited.

anesthesia measures cortical state and cortical input. J Clin Monit Comput 2018; 32:173–88
16. Kuhlmann L, Foster BL, Liley DT: Modulation of functional EEG networks by the NMDA antagonist nitrous oxide. PLoS One 2013; 8:e56434
17. Bai Y, Xia X, Li X: A review of resting-state electroencephalography analysis in disorders of consciousness. Front Neurol 2017; 8:471
18. Parameshwaran D, Subramaniyam NP, Thiagarajan TC: Waveform complexity: A new metric for EEG analysis. J Neurosci Methods 2019; 325:108313
19. Marwan N, Romano MC, Thiel M, Kurths J: Recurrence plots for the analysis of complex systems. Phys Rep 2007; 438:237–329
20. Shalbaf R, Behnam H, Sleigh JW, Steyn-Ross DA, Steyn-Ross ML: Frontal-temporal synchronization of EEG signals quantified by order patterns cross recurrence analysis during propofol anesthesia. IEEE Trans Neural Syst Rehabil Eng 2015; 23:468–74
21. Biersner RJ: Selective performance effects of nitrous oxide. Hum Factors 1972; 14:187–94
22. Biersner RJ, Hall DA, Neuman TS, Linaweaver PG: Learning rate equivalency of two narcotic gases. J Appl Psychol 1977; 62:747–50
23. Hamilton K, Laliberté MF, Heslegrave R: Subjective and behavioral effects associated with repeated exposure to narcosis. Aviat Space Environ Med 1992; 63:865–9
24. Fowler B, Granger S, Ackles KN, Holness DE, Wright GR: The effects of inert gas narcosis on certain aspects of serial response time. Ergonomics 1983; 26:1125–38
25. Vrijdag XC, van Waart H, Sleigh JW, Mitchell SJ: Pupillometry is not sensitive to gas narcosis in divers breathing hyperbaric air or normobaric nitrous oxide. Diving Hyperb Med 2020; 50:115–20
26. Klem GH, Lüders HO, Jasper HH, Elger C: The ten-twenty electrode system of the International Federation. Electroencephalogr Clin Neurophysiol 1999; 52:3–6
27. Zacny JP, Sparacino G, Hoffmann P, Martin R, Lichtor JL: The subjective, behavioral and cognitive effects of subanesthetic concentrations of isoflurane and nitrous oxide in healthy volunteers. Psychopharmacology (Berl) 1994; 114:409–16
28. Tiplady B, Degia A, Dixon P: Assessment of driver impairment: Evaluation of a two-choice tester using ethanol. Transp Res Part F Traffic Psychol Behav 2005; 8:299–310
29. Hayman MAX: Two minute clinical test for measurement of intellectual impairment in psychiatric disorders. Arch Neurol Psychiatry 1942; 47:454–64
30. Oostenveld R, Fries P, Maris E, Schoffelen JM: FieldTrip: Open source software for advanced analysis of MEG, EEG, and invasive electrophysiological data. Comput Intell Neurosci 2011; 2011:156869
31. Beim Graben P, Jimenez-Marin A, Diez I, Cortes JM, Desroches M, Rodrigues S: Metastable resting state brain dynamics. Front Comput Neurosci 2019; 13:62
32. Marwan N, Kurths J: Nonlinear analysis of bivariate data with cross recurrence plots. Phys Lett A 2002; 302:299–307
33. Dennis I, Evans JSBT: The speed–error trade-off problem in psychometric testing. Br J Psychol 1996; 87:105–29
34. Darracq M, Sleigh J, Banks MI, Sanders RD: Characterising the effect of propofol on complexity and stability in the EEG power spectrum. Br J Anaesth 2018; 121:1368–9
35. Shalbaf R, Behnam H, Sleigh J: Order patterns recurrence analysis of electroencephalogram during sevoflurane anesthesia. Biomed Eng Appl Basis Commun 2015; 27:1550049
36. Sleigh J, Warnaby C, Tracey I: General anaesthesia as fragmentation of selfhood: Insights from electroencephalography and neuroimaging. Br J Anaesth 2018; 121:233–40
37. Mashour GA, Roelfsema P, Changeux JP, Dehaene S: Conscious processing and the global neuronal workspace hypothesis. Neuron 2020; 105:776–98
38. Koch C, Massimini M, Boly M, Tononi G: Neural correlates of consciousness: Progress and problems. Nat Rev Neurosci 2016; 17:307–21
39. Acharya UR, Hagiwara Y, Deshpande SN, Suren S, Koh JEW, Oh SL, Arunkumar N, Ciaccio EJ, Lim CM: Characterization of focal EEG signals: A review. Futur Gener Comput Syst 2019; 91:290–9
40. Tripathy RK, Rajendra Acharya U: Use of features from RR-time series and EEG signals for automated classification of sleep stages in deep neural network framework. Biocybern Biomed Eng 2018; 38:890–902
41. Ma Y, Shi W, Peng CK, Yang AC: Nonlinear dynamical analysis of sleep electroencephalography using fractal and entropy approaches. Sleep Med Rev 2018; 37:85–93
42. Liu Q, Ma L, Fan SZ, Abbod MF, Shieh JS: Sample entropy analysis for the estimating depth of anaesthesia through human EEG signal at different levels of unconsciousness during surgeries. PeerJ 2018; 6:e4817
43. Nicolaou N, Georgiou J: The study of EEG dynamics during anesthesia with cross-recurrence rate. Cureus 2014; 6:e195
44. León-Domínguez U, León-Carrión J: Prefrontal neural dynamics in consciousness. Neuropsychologia 2019; 131:25–41
45. Lee U, Mashour GA: Role of network science in the study of anesthetic state transitions. Anesthesiology 2018; 129:1029–44
46. Zacharias N, Musso F, Müller F, Lammers F, Saleh A, London M, de Boer P, Winterer G: Ketamine effects on default mode network activity and vigilance: A

Downloaded from http://asa2.silverchair.com/anesthesiology/article-pdf/134/2/202/512628/20210200.0-00013.pdf by guest on 19 April 2024

Copyright © 2020, the American Society of Anesthesiologists, Inc. Unauthorized reproduction of this article is prohibited.

randomized, placebo-controlled crossover simultaneous fMRI/EEG study. Hum Brain Mapp 2020; 41:107–19
47. Lee JM, Kim PJ, Kim HG, Hyun HK, Kim YJ, Kim JW, Shin TJ: Analysis of brain connectivity during nitrous oxide sedation using graph theory. Sci Rep 2020; 10:1–11
48. Raichle ME: The brain's default mode network. Annu Rev Neurosci 2015; 38:433–47
49. Smith V, Mitchell DJ, Duncan J: Role of the default mode network in cognitive transitions. Cereb Cortex 2018; 28:3685–96
50. Murphy C, Jefferies E, Rueschemeyer SA, Sormaz M, Wang HT, Margulies DS, Smallwood J: Distant from input: Evidence of regions within the default mode network supporting perceptually-decoupled and conceptually-guided cognition. Neuroimage 2018; 171:393–401

Appendix 1. EEG Data Cleaning Script Based on FieldTrip Toolbox

```
close all
clear
clc

epochtype= 'closed end';%'math';% 'open end';

[datasetselection,datapath] = data_selector;

for i=1:length(datasetselection) %all selected data folders
    filepath=[datapath datasetselection{i} filesep];
    filelist=dir([filepath '*.bdf']);%find all.bdf files

    %creating folder for cleaned files to be stored
    newfilepath=[filepath filesep 'cleaned' filesep];
    mkdir(newfilepath);

    for j=2:length({filelist.name}) % all BDF files in the folder

        %define epoch trial data
        cfg = [];
        cfg.dataset = [filepath filelist(j).name];
        cfg.trialfun = 'EEG_trialfunc_narcosis'; % my function to read epochtimes from excel file
        cfg.trialdef.epochtype = epochtype;
        cfg.trialdef.pretrial = 1; % add sec of data before trial
        cfg.trialdef.posttrial = 1; % add sec of data after trial
        cfg = ft_definetrial(cfg);

        %read dataset based on trial definition
        cfg.channel = 1:34;
        cfg.reref = 'yes';
        cfg.refchannel = 'EEG'; % average of all EEG channels
        cfg.demean = 'yes';
        cfg.detrend = 'yes';
        data = ft_preprocessing(cfg);

        % downsample data
        cfg = [];
        cfg.resamplefs = 256; %Hz
        data = ft_resampledata(cfg, data);

        % removing line and low freq noise
        cfg = [];
        cfg.channel = 'all';
        cfg.bsfilter = 'yes'; % band-stop method
        cfg.bsfreq = [49 51];
        cfg.hpfilter = 'yes';
        cfg.hpfreq = 1; % removing all activity below 1 Hz
        data = ft_preprocessing(cfg,data);

        % clean high harmonic of line noise
        cfg=[];
        cfg.channel = channels;
        cfg.bsfilter = 'yes'; % band-stop method
        cfg.bsfreq = [99 101];
        cfg.demean = 'yes';
        cfg.detrend = 'yes';
        data = ft_preprocessing(cfg,cleandata);

        % calculate ICA components to project out eye and cardiac artefacts
        cfg = [];
        cfg.method = 'runica';
        comp = ft_componentanalysis(cfg, data);

        cfg = [];
        cfg.layout = 'biosemi32.lay';
        cfg.viewmode = 'component';
        cfg.ylim = [-0.0002 0.0002];
        cfg.zlim = 'maxmin';
        cfg.compscale = 'local'; % scale each component separately
        cfg.blocksize = 62;
        cfg.artifactalpha = 0.8;
        cfg.position = [0 0 3000 2000];
        ft_databrowser(cfg, comp);

        % calculating properties to suggest, select and reject bad components
        EOG_chans = [33 34];
        [bad_comps,reasons] = ICAbadICdetection(data,comp, EOG_chans);
        for k=1:length(bad_comps)
        ft_info('Suggested bad component: %d because of %s',bad_comps(k),reasons{k})
        end
        ic.artifact = input('ICs to reject (i.e. [8] or 0 for all suggested bad components):');

        if ic.artifact==0
        ic.artifact=bad_comps;
        end
```

Downloaded from http://asa2.silverchair.com/anesthesiology/article-pdf/134/2/202/512628/20210200.0-00013.pdf by guest on 19 April 2024

Copyright © 2020, the American Society of Anesthesiologists, Inc. Unauthorized reproduction of this article is prohibited.

```
        cfg = [];
        cfg.component = ic.artifact;
        data = ft_rejectcomponent(cfg, comp, data);

        % remove padding of 1 sec before and after and correct time axes
        cfg = [];
        cfg.toilim = [1 data.time{1,1}(end)-1];
        data = ft_redefinetrial(cfg, data);
        cfg = [];
        cfg.offset = -data.fsample;
        data = ft_redefinetrial(cfg, data);

        %cut in 2 second "trials"
        cfg = [];
        cfg.length = 2;
        cfg.overlap = 0;
        data_segmented = ft_redefinetrial(cfg, data);

        % detect artefacts
        cfg=[];
        cfg.artfctdef.eog.channel = {'EXG1','EXG2'};
        cfg.artfctdef.eog.cutoff = 7;
        cfg.artfctdef.muscle.channel = 'EEG';
        cfg.artfctdef.muscle.bpfreq = [105 120];
        cfg.artfctdef.muscle.cutoff = 10;
        [cfg,~] = ft_artifact_eog(cfg, data_segmented);
        [cfg,~] = ft_artifact_muscle(cfg, data_segmented);

        %visually inspect data and defined artefacts
        cfg.channel = 'all';
        cfg.viewmode = 'vertical';
        cfg.ylim = [-40 40];
        cfg.position = [0 0 3000 2000];
        cfg.blocksize = 10; % time window to browse
        cfg.artifactalpha = 0.8; % this make the colors less transparent and thus more vibrant
        cfg = ft_databrowser(cfg, data);

        %rejecting trials with artefacts
        cfg.artftdef.reject = 'complete';
        cleandata=ft_rejectartifact(cfg,data_segmented);

        %store cleaned data
        [~,newfilename,~]=fileparts(filelist(j).name);
        newfilename=['CLEAN' newfilename ' ' epochtype '.mat'];
        save(strcat(newfilepath,newfilename),'cleandata','-v7.3')
    end
end
```

Supporting Functions

```
function[bad_comps,reasons]=ICAbadICdetection(data,comp,EOG_chans)
% ICA bad components detection function
% detection scripts are from the FASTER toolbox
% utilising functions from the EEGlab toolbox
list_properties = component_properties(data,comp,EOG_chans);
rejection_options.measure=ones(1,size(list_properties,2));%use all properties
rejection_options.z=3*ones(1,size(list_properties,2));%z-value of 3 for each property

[lengths,all_l] = min_z(list_properties,rejection_options);
bad_comps=find(lengths);
properties={'High freq noise''Kurtosis''Hurst''Eyeblink'};
for i=1:length(bad_comps)
reasons{i}=cell2str(properties(all_l(bad_comps(i),:)));
end
end

function string1 = cell2str(cellarray)
string1=[];
for i=1:length(cellarray)
    string1=[string1 cellarray{i}];
    if length(cellarray)>i
        string1=[string1 ' & '];
    end
end
end
function list_properties = component_properties (data,comp,blink_chans)
list_properties = zeros(size(comp.trial,1),4); %This 4 corresponds to number of properties.

for u=1:size(comp.trial{1},1)
    measure = 1;
    % TEMPORAL PROPERTIES

    % Median gradient value, for high frequency artefacts
    list_properties(u,measure) = median(diff(comp.trial{1}(u,:)));
    measure = measure + 1;

    % SPATIAL PROPERTIES

    % Kurtosis of spatial map (if v peaky, i.e. one or two points high
    % and everywhere else low, then it's probably noise on a single
    % channel)
    list_properties(u,measure) = kurt(comp.topo(:,u));
    measure = measure + 1;

    % OTHER PROPERTIES

    % Hurst exponent - detects nonphysiological signals
    list_properties(u,measure) = hurst_exponent(comp.trial{1}(u,:));
    measure = measure + 1;

    % Eyeblink correlations
    if (exist('blink_chans','var') && ~isempty(blink_chans))
        for v = 1:length(blink_chans)
            if ~(max(data.trial{1}(blink_chans(v),:))==0 && min(data.trial{1}(blink_chans(v),:))==0)
```

Downloaded from http://asa2.silverchair.com/anesthesiology/article-pdf/134/2/202/512628/20210200.0-00013.pdf by guest on 19 April 2024

Copyright © 2020, the American Society of Anesthesiologists, Inc. Unauthorized reproduction of this article is prohibited.

```
            f = corrcoef(comp.trial{1}(u,:),data.trial{1}(blink_chans(v),:));
            x(v) = abs(f(1,2));
        else
            x(v) = v;
        end
    end
    list_properties(u,measure) = max(x);
    measure = measure + 1;
    end
end

for u = 1:size(list_properties,2)
    list_properties(isnan(list_properties(:,u)),u)=nanmean(list_properties(:,u));
    list_properties(:,u) = list_properties(:,u) - median(list_properties(:,u));
end
end

function[lengths,all_l]=min_z(list_properties,rejection_options)
rejection_options.measure=logical(rejection_options.measure);
zs=list_properties-repmat(mean(list_properties,1),size(list_properties,1),1);
zs=zs./repmat(std(zs,[],1),size(list_properties,1),1);
zs(isnan(zs))=0;
all_l = abs(zs) > repmat(rejection_options.z,size(list_properties,1),1);
lengths = any(all_l(:,rejection_options.measure),2);
end
```

Appendix 2. Complexity Script

```
close all; clear; clc

%settings
Ts=0.25; %duration of sample in sec
RQAselect=3; % entropy
Rnpercentile=50; % percentile for threshold
channels= 1:32;

%select dataset
%for model figure select participant 1
[datasetselection,datapath] = data_selector;
epochtype= 'open end'; % 'closed end';% 'math'; % 'open end'; %
exposures={'baseline''20%''30%''40%''final'};

for k=1:length(datasetselection) %all selected data folders
    filepath=[datapath datasetselection{k} filesep 'cleaned' filesep];

    RnThreshold=[];
    for l=1:length(exposures) % loop over all exposures
        % load datafile

        filename=['CLEAN' datasetselection{k} ' ' exposures{l} ' ' epochtype '.mat'];
        load([filepath filename])

    % split previously defined trials (2 second) into smaller samples
        a=1;
        samples=[];
        N=Ts*data.fsample;
        for i=1:length(data.trial)
            for j=1:(floor(length(data.trial{1})/N))
                samples(a,:,:)=data.trial{i}(:,1+(j-1)*N:N*j);
                a=a+1;
            end
        end

        %DIMORD samples = samples * channels * time

        % calculate the Pierson correlation between the samples for all channels
        Rn=[];
        for i=1:size(samples,2)
            Rn(i,:,:)=corr(squeeze(samples(:,i,:))');
        end

        % convert the correlation values
        Rn=abs(Rn);

        % set threshold at baseline exposure for all exposures for each defined percentile
        if l==1
            RnT=Rn;
            RnT(RnT==0)=NaN;
            RnThreshold=prctile(reshape(RnT,1,[]),Rnpercentile);
        end

        % Convert to logical values based on threshold
        RnLogic = (Rn > RnThreshold);
        %calculate the defined RQA metrics for each channel
        for i=1:size(RnLogic,1)
            RQresults(k,l,i) = Recu_RQA(squeeze(RnLogic(i,:,:)),1,RQAselect);
        end

        %DIMORD RQresults participants, exposures, channels

        % calculate DMN complexity: median of the region of
        % interest which are the electrodes that have entropy >1 at baseline
            if l==1
        DMN=find(RQresults(k,l,:)>1);
        end
        DMNcomplexity(k,l)=median(RQresults(k,l,DMN));
        % DIMORD participants, exposures
    end
end
```

Supporting Functions

```
function [RQA] = Recu_RQA(RP,I,metrics)

% Recurrence quantification analysis of recurrence plots
```

Downloaded from http://asa2.silverchair.com/anesthesiology/article-pdf/134/2/202/512628/20210200.0-00013.pdf by guest on 19 April 2024

Copyright © 2020, the American Society of Anesthesiologists, Inc. Unauthorized reproduction of this article is prohibited.

```
% RP: the Recurrence Plot
% I: the indication marks (I=0 RP is the symmetry matrix
%                          I=1 RP is the asymmetry matrix)
%outputs in RQA
% 1 RR: Recurrence rate RR, The percentage of recurrence points in an RP
% Corresponds to the correlation sum;
% 2 DET: Determinism DET,The percentage of recurrence points which form
% diagonal lines
% 3 ENTR: Entropy ENTR, The Shannon entropy of the probability distribution of the diagonal
% line lengths p(l)
% 4 L: Averaged diagonal line length L, The average length of the diagonal lines
% 5 LAM: Laminnarity, The percentage of recurrence points which form vertical lines
% 6 TT: Trapping time, The average length of the vertical lines
% 7 Clust:global clustering coefficient, Network analysis
% 8 Trans:Transitivity, Network analysis

% If you need these codes that implement critical functions with (fast) C code, please visit my website:
% http://www.escience.cn/people/gxouyang/Tools.html

% revise time: May 5 2014, Ouyang,Gaoxiang
% Email: ouyang@bnu.edu.cn

%% minimal length of diagonal and vertical line structures
Lmin=2; %diagonal
Vmin=2; %vertical
if nargin < 2
    I=0;
end

%% calculate diagonals
N1=size(RP,1);

Yout=zeros(1,N1);

for k=2:N1
    On=1;
    while On<=N1+1-k
        if RP(On,k+On-1)==1
            A=1;off=0;
            while off==0 & On~=N1+1-k
                if RP(On+1,k+On)==1
                    A=A+1;On=On+1;
                else
                    off=1;
                end
            end
            Yout(A)=Yout(A)+1;
        end
        On=On+1;
    end
end

if I==0
    S=2*Yout;
end
if I==1
    RP=RP';
    for k=2:N1
        On=1;
        while On<=N1+1-k
            if RP(On,k+On-1)==1
                A=1;off=0;
                while off==0 & On~=N1+1-k
                    if RP(On+1,k+On)==1
                        A=A+1;On=On+1;
                    else
                        off=1;
                    end
                end
                Yout(A)=Yout(A)+1;
            end
            On=On+1;
        end
    end
    S=Yout;
end

%% calculate the recurrence rate (RR)
SR=0;
for i=1:N1
        SR=SR+i*S(i);
end
RR=SR/(N1*(N1-1));

%% calculate the determinism (%DET)
if SR==0
    DET=0;
else
        DET=(SR-sum(S(1:Lmin-1)))/SR;
end

%% calculate the ENTR = entropy (ENTR)
pp=S/sum(S);
entropy=0;
F=find(S(Lmin:end));
l=length(F);
if l==0
    ENTR=0;
else
    F=F+Lmin-1;
    ENTR=-sum(pp(F).*log(pp(F)));
end

%% calculate Averaged diagonal line length (L)
L=(SR-sum([1:Lmin-1].*S(1:Lmin-1)))/sum(S(Lmin:end));

%% calculate Laminarity (LAM) and Trapping time (TT) (Marwan et al. 2002)
[~, d, ~]=tt(RP);
```

Downloaded from http://asa2.silverchair.com/anesthesiology/article-pdf/134/2/202/512628/20210200.0-00013.pdf by guest on 19 April 2024

Copyright © 2020, the American Society of Anesthesiologists, Inc. Unauthorized reproduction of this article is prohibited.

```
d(d<Vmin)=[];
if sum(RP(:))>0
    LAM=sum(d)/sum(sum(RP));
else
    LAM=NaN;
end
TT=mean(d);

%% network measures
% global clustering coefficient (Marwan et al., 2009)
kv = sum(RP,1); % degree of nodes
Clust = nanmean(diag(double(RP)*double(RP)*double(RP))' ./ (kv.* (kv-1)));
% transitivity
denom = sum(sum(double(RP) * double(RP)));
Trans = trace(double(RP)*double(RP)*double(RP))/denom;

aa=1;
if ismember(1,metrics);RQA(aa)=RR;aa=aa+1;end
if ismember(2,metrics);RQA(aa)=DET;aa=aa+1;end
if ismember(3,metrics);RQA(aa)=ENTR;aa=aa+1;end
if ismember(4,metrics);RQA(aa)=L;aa=aa+1;end
if ismember(5,metrics);RQA(aa)=LAM;aa=aa+1;end
if ismember(6,metrics);RQA(aa)=TT;aa=aa+1;end
if ismember(7,metrics);RQA(aa)=Clust;aa=aa+1;end
if ismember(8,metrics);RQA(aa)=Trans;end
```

ANESTHESIOLOGY REFLECTIONS FROM THE WOOD LIBRARY-MUSEUM

Life from Death: The Tragedy and Heroism of Dr. Paluel J. Flagg

As a young physician in New York City, Paluel J. Flagg, M.D. (1886 to 1970, *right*), lost his daughter to neonatal asphyxia in 1912. His wife also died that year. Grief-stricken, Dr. Flagg found solace in easing human suffering, and began treating leprosy patients in Haiti. In 1912, he also committed his life to the prevention and treatment of asphyxia. What better profession to accomplish this than anesthesiology? In his landmark textbook *The Art of Anesthesia* (1916), Flagg presaged the modern intensive care unit by calling anesthesiologists *pneumatologists*—respiratory experts who should extend their practice beyond the operating room. Naturally, Flagg took to refining devices for airway management. He introduced his two-piece metal endotracheal tube (*left*) in 1928. Spiral wires made the outer catheter flexible, and a rigid inner stylet prevented kinking during insertion. Later, Flagg would develop the first laryngoscope with batteries in the handle. As founder of the National Resuscitation Society and the Society for the Prevention of Asphyxial Death, the heroic physician taught resuscitation maneuvers to countless doctors and paramedics. A good friend of aviator Charles Lindbergh, Flagg, when his soul flew to the heavens, left behind a legacy of patient safety and abundant living progeny—8 sons, 4 daughters, 56 grandchildren, and 3 great-grandchildren. (Copyright © the American Society of Anesthesiologists' Wood Library-Museum of Anesthesiology, Schaumburg, Illinois.)

Jane S. Moon, M.D., University of California, Los Angeles, and Melissa L. Coleman, M.D., Penn State College of Medicine, Hershey, Pennsylvania.

Downloaded from http://asa2.silverchair.com/anesthesiology/article-pdf/134/2/202/512628/20210200.0-00013.pdf by guest on 19 April 2024

Copyright © 2020, the American Society of Anesthesiologists, Inc. Unauthorized reproduction of this article is prohibited.